


SCIENTIFIC REPORTS



OPEN

Significant production of humic fluorescent dissolved organic matter in the continental shelf waters of the northwestern Pacific Ocean

Jeonghyun Kim , Hyung-Mi Cho & Guebuem Kim

Fluorescent dissolved organic matter (FDOM) is important for marine organisms and the global carbon cycle contributing to the optical properties of surface seawater and organic carbon budgets. Rivers are known to be the main source of FDOM in coastal oceans and marginal seas. In this study, however, we show that the contribution of FDOM produced from organic sediments of the northwestern Pacific continental shelf is similar to that from the Changjiang River. FDOM showed relatively higher concentrations at stations off the Changjiang River mouth and in the central Yellow Sea. Based on temperature-salinity diagrams, the major source of surface FDOM in summer surface waters was found to be from the Changjiang River while that observed in the winter water column was produced mainly in the continental shelf. A good correlation between ^{228}Ra and the humic-like FDOM (FDOM_h) during the winter suggests that the FDOM_h is produced mainly from marine sediments and enriched in water over the water residence times. A simple mass balance calculation shows that the excess FDOM_h fluxes produced from marine sediments account for 30–40% of the riverine source. This result suggests that the continental shelf is an important hidden source of FDOM in the upper ocean.

Colored dissolved organic matter (CDOM) is the light-absorbing fraction of reduced organic matter in aquatic environments. A part of CDOM, which is also fluorescent over a wide wavelength range after absorbing energy, is traditionally termed as fluorescent dissolved organic matter (FDOM). Thus, FDOM has a direct influence on underwater light fields, especially absorbing ultraviolet and visible radiation^{1–4}. These also impact the marine chemical cycles in terms of the production of greenhouse gases (e.g., carbonyl sulfide, CO, and CO₂), speciation of trace metals, and bioavailability of organic substrates through a variety of photochemical reactions^{4–6}. FDOM has been used as an indicator of dissolved organic matter (DOM) and dissolved organic carbon (DOC) in the ocean because most DOM show distinct optical signals.

In coastal oceans and marginal seas, rivers are known to be the major source of FDOM as significant negative relationships between FDOM and salinity and lignin have been observed^{7,8}. However, recent studies have suggested that sinking organic matter and bottom sediments could also be a significant source of FDOM in the ocean^{9–12}. Yamashita and Tanoue¹³ showed that *in situ* production of FDOM in the interior of the Pacific Ocean is almost five times greater than global riverine inputs of terrestrial FDOM. As such, Kim and Kim¹⁴ showed that the deep-sea production of humic-like FDOM accounts for 20–30% of the riverine flux in the surface ocean of the East Sea (Sea of Japan). More recently, Kim and Kim⁹ showed significant excess humic-like FDOM inputs from bottom sediments based on apparent oxygen utilization (AOU) and FDOM correlations. They showed that approximately 10% of the humic-like FDOM in the deep ocean (1000 m – bottom) can be introduced from the anoxic layer of bottom sediments in the East Sea⁹.

The northwestern Pacific continental shelf (approximately 1 million km² area), including the Yellow Sea, the East China Sea, the southern sea off Korea, and the East Sea, is one of the largest continental shelves in the world¹⁵ (Fig. 1). The Kuroshio branch water, which is a strong western boundary current, flows into the northwestern

School of Earth and Environmental Sciences, Seoul National University, 1 Gwanak-ro, Gwanak-gu, Seoul, 08826, Korea. Correspondence and requests for materials should be addressed to G.K. (email: gkim@snu.ac.kr)

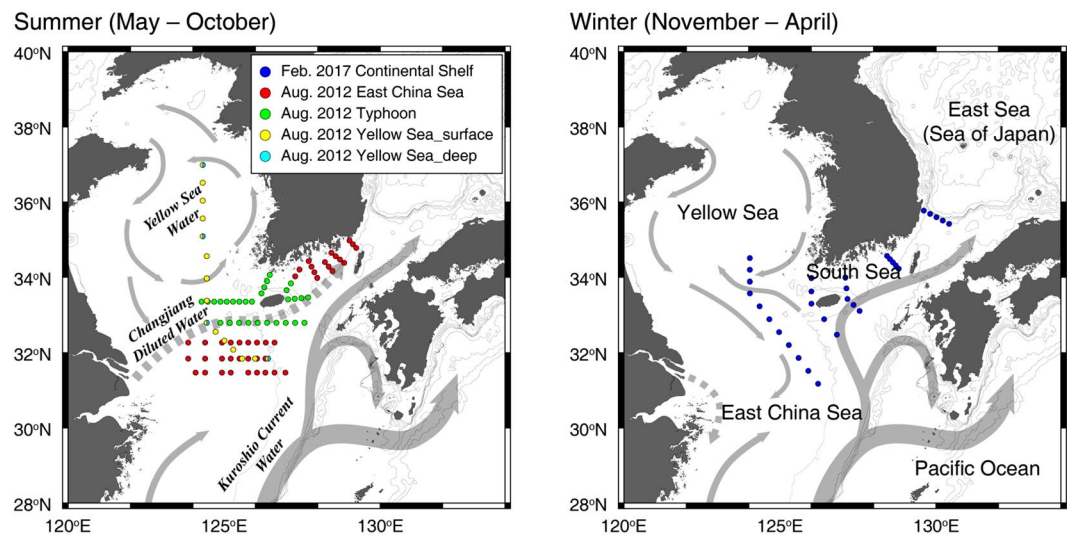


Figure 1. Maps showing sampling stations, bottom topography, and schematics patterns of surface currents on the northwestern Pacific continental shelf during the summer and winter sampling periods. The solid arrows represent the seawater current, and the dotted arrows represent the Changjiang Diluted Water (CDW) current. The maps were created using Ocean Data View software version 4.7.10. (<https://odv.awi.de>) and the sampling stations and current patterns were drawn using Adobe Illustrator CC software version 2015.0.1. (<http://www.adobe.com/>).

Pacific continental shelf and the East Sea¹⁶. Here, the branch of the Kuroshio Current is mixed with the river waters and the continental shelf water, thereby supplying high concentrations of terrestrial organic matter and inorganic nutrients. During the warm season (from May to November), the vertical temperature gradient and the freshwater discharge induce a strong pycnocline (surface layer of 10 m)¹⁷, while it is fully mixed during the cold season (from December to April)¹⁷. In particular, this continental shelf contains high concentrations of sedimentary organic matter with fine-grained sediments from the Changjiang (Yangtze) and Yellow rivers. The Changjiang River, which is one of the world's largest rivers, is the dominant source of freshwater ($\sim 9 \times 10^2 \text{ km}^3/\text{year}$; approximately 90% of total river discharge) in this region^{16,18,19}. The freshwater plume originating from the Changjiang River extends southward along the Zhejiang coast during the winter and northeastward to the East Sea through the Korea-Tsushima Strait during the summer^{16,18,20}. After the construction of the Three Gorges Dam in 2003, the sediment load decreased by approximately 30%²¹, while no significant long-term variations in the annual freshwater discharge were observed^{22–24}.

The distribution characteristics of FDOM in this region were recently investigated by analyzing the absorption and fluorescence of DOM. Guo *et al.*²⁵ reported the conservative and non-conservative distribution behaviors of CDOM versus salinity in Chinese estuaries. Bai *et al.*²⁶ and Su *et al.*²⁷ investigated the factors contributing to the spatial and seasonal distributions of FDOM in the southern Yellow Sea and the East China Sea using the fluorescence index and the relationships between FDOM components and certain parameters (Chl-a, AOU, and salinity) indicating potential sources.

In this study, we examined the relative contributions of FDOM production from organic sediments compared with those from riverine inputs based on the hypothesis that organic-rich continental shelf sediments can effectively produce FDOM for the shallow water column. We used specific hydrological properties based on the temperature-salinity (T-S) diagram and ²²⁸Ra as tracers to differentiate different sources of FDOM in the region.

Results and Discussion

Identification of FDOM components. Three FDOM components were characterized using the Parallel Factor Analysis (PARAFAC) model (Figure S1). Briefly, Component 1 (C1, Ex/Em = 325/392 nm) is traditionally referred to as the marine humic-like FDOM component (FDOM_H), M peak²⁸. It is known to be derived mainly from microbial-derived fulvic acids²⁸. Murphy *et al.*²⁹ also reported that this component is *in-situ* produced from terrestrial and marine organic substrates and is a newly-produced organic matter regardless of its origin. The C1 can be produced by the shift of the peak position to shorter wavelengths (“blue-shift”) from C peak showing longer wavelengths. Component 2 (C2, Ex/Em = 285/332 nm) is identified as the tryptophan amino acid-like and protein-like FDOM component (FDOM_P), T peak²⁸. It is known to originate from polyphenolic- or protein-like materials derived from freshly produced organic matter³⁰. Thus, the relatively high concentrations of FDOM_P were observed in regions where biological activity is relatively high in the surface ocean^{31,32}. The FDOM_P can also originate from anthropogenic sewage and farm wastes³². Component 3 (C3, Ex/Em = 385/448 nm) is the terrestrial FDOM_H component, C peak, which has longer excitation and emission wavelengths compared to those of C1²⁸. Its red-shifted peak location is known to be associated with its condensed molecular structures, indicating that the fluorescent signal of C3 is linked to terrestrial detrital DOM produced by degradation of higher plants³⁵.

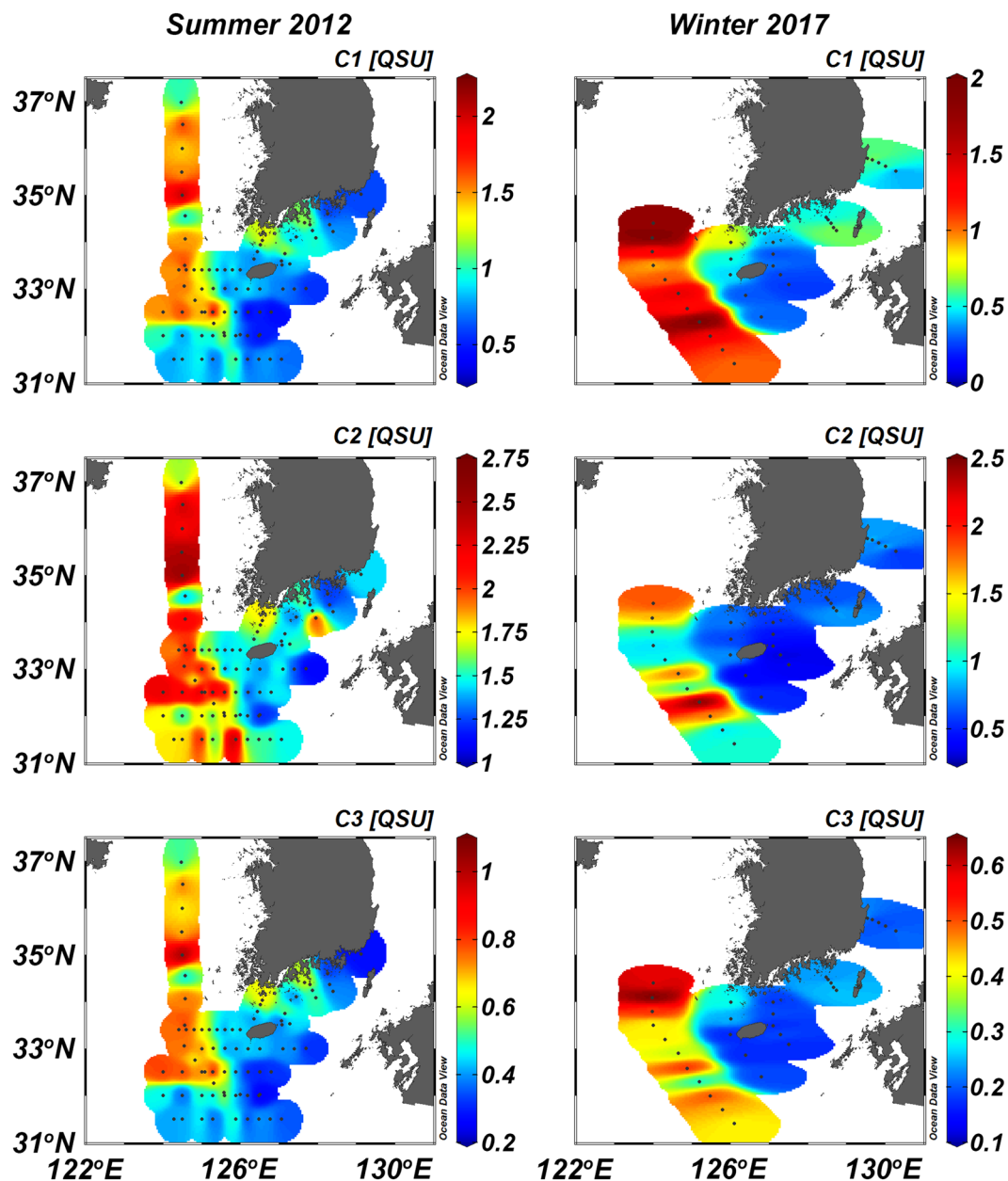


Figure 2. Contour figures of FDOM components, C1, C2, and C3, in surface waters of the northwestern Pacific continental shelf during the summer of 2012 and winter of 2017. The contour plots were created using Ocean Data View software version 4.7.10. (<https://odv.awi.de>).

In addition, the production of C3 from marine organic matter is observed in the global deep ocean³⁴. Thus, in this study, we do not differentiate C1 and C3 explicitly, and simply regard them as different components of FDOM_H.

The origins of FDOM in the ocean. The concentrations of the three FDOM components in surface water were relatively higher at stations off the Changjiang River mouth and in the central Yellow Sea during the summer (Fig. 2). The average concentrations of FDOM in the surface water of the continental shelf (1.0 ± 0.4 QSU for C1; 1.7 ± 0.3 QSU for C2; and 0.5 ± 0.2 QSU for C3) were approximately two times higher than those at the highest salinity station (0.5 QSU for C1; 1.1 QSU for C2; and 0.3 QSU for C3) in the East China Sea, which is considered as a branch of the oligotrophic Kuroshio Current water (Figs 2 and 3). FDOM concentrations were negatively correlated to salinities (Fig. 3). The distribution of FDOM and its relationship to salinity during the summer indicate that FDOM, regardless of its properties, originates mainly from the Changjiang River¹⁴. Based on the potential T-S diagram for the summer, the distributions of all FDOM components in the surface continental shelf waters showed mixing patterns between the Changjiang Diluted Water (CDW) and the oligotrophic Kuroshio Surface Water (KSW) (Figure S2). This pattern is related to the Changjiang River plume extending northeastward to the East Sea over the continental shelf region during the summer. Changjiang River water contains high

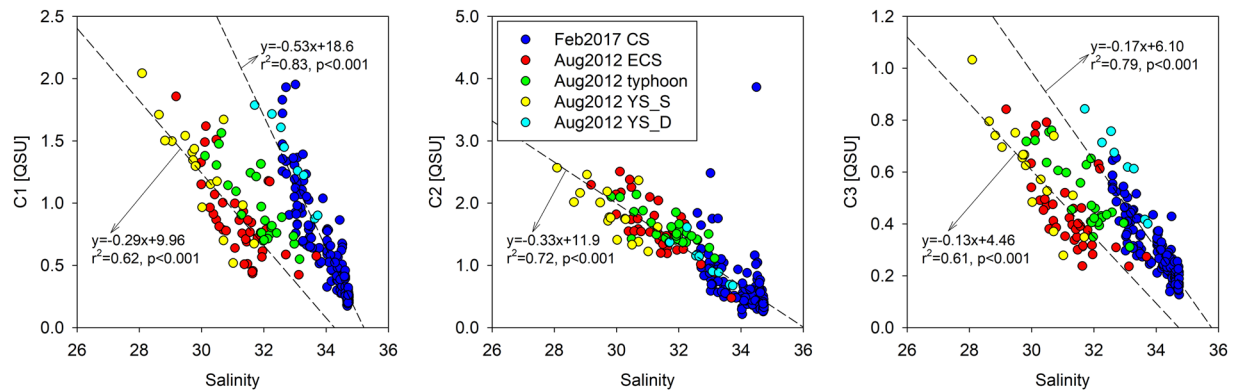


Figure 3. Scatterplots of FDOM concentrations versus salinities in the continental shelf waters during the summer of 2012 and winter of 2017. Correlation coefficients between FDOM_H and salinity were evaluated from the data for the surface FDOM during August 2012, except for the post-typhoon period, and for the winter of 2017 and from the deep FDOM of the Yellow Sea during August 2012.

concentrations of inorganic nutrients as well as terrestrial organic matter³⁵. Efflux of enriched fulvic and humic acids from soils and *in situ* biological degradation of organic matter in the river water may contribute to high concentrations of riverine FDOM_H^{26,33,36}. In addition, river-driven organic and inorganic nutrients could result in active biological production of FDOM_p at the river mouth.

During February 2017, the relationship between FDOM and salinity also showed negative trends (Fig. 3). However, these distribution patterns seem to be independent of the direct Changjiang River discharge as the influence of CDW on the study region is minor during the winter (Figure S2)³⁷. This hypothesis is supported by the sectional distributions of the FDOM components across the continental shelf from the Yellow Sea to the southern East China Sea during February 2017, showing an increase in FDOM toward the central Yellow Sea (Figures S2; S3). Furthermore, the winter T-S diagram shows that the FDOM distributions are dependent on the mixing between the Yellow Sea Bottom Water (YSBW) and the Kuroshio Tropical Water (KTW). The concentrations of FDOM_H during February 2017 were much higher than those expected from the FDOM_H-salinity correlation observed during August 2012 (Fig. 3). The excess FDOM_H, which is in excess of that contributed by the Changjiang River, is consistent with a significant enrichment of FDOM_H in the deep-water layer of the Yellow Sea observed during August 2012 for the same salinity waters (Fig. 3).

There are three possible processes that influence the enrichment of high FDOM_H in the YSBW: 1) inputs from other smaller rivers, 2) submarine fresh groundwater discharge, and 3) *in situ* microbial production or diffusive and advective fluxes from bottom sediments and pore waters. Smaller river and fresh groundwater inputs can be excluded from the major source of deep FDOM_H because the Changjiang River is the dominant freshwater source (more than 90%). Even if they are significant, these freshwater-origin FDOM_H samples should be shown in the T-S diagram. However, we cannot differentiate internal sources from the sinking particles and bottom organic sediments, which can gradually enhance FDOM_H in deep water over time. We do not use AOU as an indicator for *in situ* production as it is not conservative in these seasonally mixed shelf waters.

Instead, we use ²²⁸Ra as a tracer of the YSBW because the large enrichment of ²²⁸Ra by diffusion from bottom sediments has been well documented and it has been utilized as a tracer of water residence times in the Yellow Sea^{38,39}. In general, ²²⁸Ra is very soluble in seawater, and ²²⁸Ra (half-life: 5.75 years) in the YSBW is produced mainly from particle-reactive ²³²Th (half-life: 1.4×10^{10} years) in bottom sediments over the water residence time. The ²²⁸Ra inputs from rivers and submarine groundwater discharge, relative to the benthic fluxes, are known to be relatively small³⁹. Because of this, long-lived ²²⁶Ra has been used for tracing groundwater inputs as the production of ²²⁶Ra (half-life: 1622 years) from particle-reactive ²³⁰Th (half-life: 7.5×10^4 years) in the surface sediments is relatively negligible^{38–41}. In this region, higher concentrations of FDOM_H were generally observed in pore waters⁴². Thus, we hypothesized that the excess FDOM_H and ²²⁸Ra in the deep layer are continuously produced from bottom sediments and accumulate in the bottom water layer over water residence times of approximately five years^{38,40}. The inputs of FDOM_H and ²²⁸Ra produced from bottom sediments through saline groundwater recirculation and those produced from sinking particles are also included in the estimation. The concentrations of FDOM_H produced in the continental shelf showed a good positive correlation with ²²⁸Ra activities soon after the strong typhoon period and the winter (February 2017) (Fig. 4). This trend suggests that the main source of the enriched FDOM_H in the YSBW is produced in the continental shelf sediment. The enriched deep FDOM_H seems to be well mixed vertically with the surface water because of winter mixing and the typhoon event (Fig. 5). However, no significant correlation was observed between FDOM_H and ²²⁸Ra in the well-stratified surface water layer during the summer of 2012, due to different source inputs between FDOM_H and ²²⁸Ra (Fig. 4).

In our study region, C2 showed a good correlation with salinities across all seasons, without seasonal changes. In general, FDOM_p in the river waters known to be derived from terrestrial sources, anthropogenic protein pollution, and local biological production in combination⁴³. The Changjiang River is the major source of nutrients and organic substances in this study region throughout the year^{44,45}. Thus, the linear trend of FDOM_p versus salinity seems to be due to significant biological production in the Changjiang River, relative to that in the continental

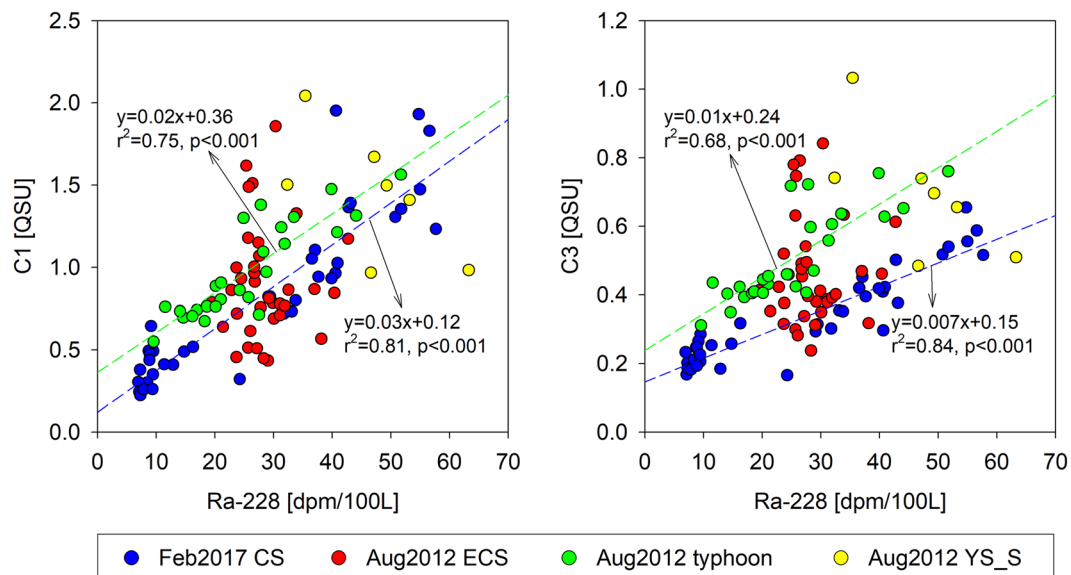


Figure 4. Scatterplots of C1 and C3 concentrations versus the activities of ^{228}Ra in the continental shelf waters during the summer of 2012 and winter of 2017.

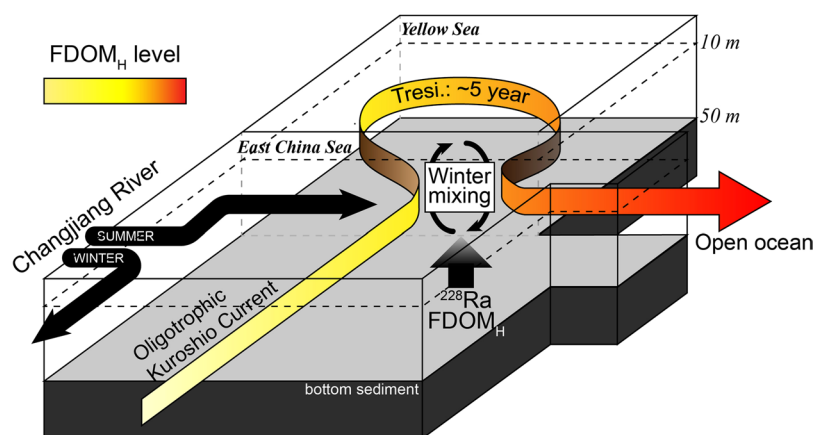


Figure 5. A schematic diagram illustrating the process of the enrichment of FDOM_H in the northwestern Pacific continental shelf waters.

shelf waters. This trend suggests that photo-bleaching and/or *in situ* production is insignificant during the estuarine mixing processes.

Estimating the fluxes of FDOM from organic sediments versus rivers. The fluxes of FDOM_H produced in the bottom water (Flux_s) can be calculated using the following equation:

$$\text{Flux}_s = \frac{(\text{FDOM}_{\text{YSBW}} - \text{FDOM}_{\text{SSYW}}) \times V_{\text{YS}}}{T_{\text{YS}}}$$

where $\text{FDOM}_{\text{YSBW}}$ and $\text{FDOM}_{\text{SSYW}}$ are the endmember values of FDOM (unit: $\mu\text{g QS/L}$) in the YSBW and the summer surface Yellow Sea water (SSYW), respectively; V_{YS} is the total water volume (unit: km^3) of the Yellow Sea; and T_{YS} is the water residence time of the Yellow Sea (unit: year). The area of the Yellow Sea is $4 \times 10^5 \text{ km}^2$, and the mean depth is 50 m³⁸. The values of $\text{FDOM}_{\text{YSBW}}$ were assumed to be $1.8 \pm 0.1 \text{ QSU}$ for C1 and $0.7 \pm 0.1 \text{ QSU}$ for C3, the average of high concentrations of FDOM_H in the deep Yellow Sea, based on the cross-sectional distributions of FDOM on the continental shelf (Figures S2 and S3). The values of $\text{FDOM}_{\text{SSYW}}$ were assumed to be 0.9 QSU for C1 and 0.5 QSU for C3, the estimated concentrations of FDOM in the surface Yellow Sea during the summer at the representative salinity of the Yellow Sea water mass ($31.5^{39,40}$) based on the correlation equation (Figure S4). Then, the fluxes of FDOM_H from organic sediments (Flux_s) were estimated to be $3.7 (\pm 0.4) \times 10^{15}$ and $1.0 (\pm 0.3) \times 10^{15} \mu\text{g QS/year}$ for C1 and C3, respectively. In this region, the FDOM fluxes from the Changjiang River were estimated to be 8.8×10^{15} and $3.8 \times 10^{15} \mu\text{g QS/year}$ for C1 and C3, respectively, by multiplying the

extrapolated intercept of the FDOM_H -salinity relationship and annual river discharge¹⁴. Therefore, FDOM_H production in the continental shelf corresponds to 42% (C1) and 26% (C3) of that from the Changjiang River which is known to be the major FDOM_H source in this study region¹⁴.

In addition to the winter mixing process, typhoons may introduce bottom source FDOM_H to the surface water during the summer. After Typhoon, Bolaven, the excess FDOM_H , relative to that expected from the measured salinity using the FDOM_H -salinity relationship before the typhoon event, was also observed in the surface water (Fig. 3). Based on the salinity- FDOM_H regression equation for the normal period, the average excess concentrations of C1 and C3 during the post-typhoon period were approximately 0.2 ± 0.2 QSU and 0.1 ± 0.1 QSU, respectively. Such FDOM increases following typhoon events are consistent with previous observations in the North Atlantic after Hurricane Gert in September 1999⁴⁶ and the Mid-Atlantic Bight after hurricane-induced vertical mixing⁴⁷. Therefore, either winter or summer mixing by special events can introduce a significant amount of bottom-sourced FDOM into surface waters, which may significantly affect carbon cycles and marine ecosystems.

Conclusions

The Changjiang River seems to be the major source of FDOM over the northwestern Pacific continental shelf surface waters during the summer. In addition, there is significant input of FDOM from organic sediments resulting in large excess FDOM_H during the winter and following typhoon events in surface waters. These bottom source inputs were proven by significant correlations between ²²⁸Ra and excess FDOM_H concentrations. The fluxes of C1 and C3 from organic sediments account for approximately 42% and 26%, respectively, of those originating from the Changjiang River. Our results highlight that the enrichment of FDOM by organic sediment sources can be a key factor controlling the distributions and fluxes of FDOM in the northwestern Pacific continental shelf. Further studies are necessary to investigate the fluxes of FDOM across the continental shelf to the open ocean.

Materials and Methods

Sampling. The winter seawater sampling was carried out in the East China Sea from 6 to 17 February 2017 aboard R/V *Onnuri* of the Korean Institute of Ocean Science and Technology (KIOST). The summer seawater sampling for deep FDOM was carried out in the Yellow Sea from 13 to 15 August 2012 aboard *KCG vessel 3011* of the Korea Coast Guard (KCG) (Fig. 1). Seawater samples were collected using 10-L Niskin bottles mounted on a CTD rosette sampler. The hydrographic data were measured using an SBE911-plus CTD profiler (Sea-Bird Electronics Inc., WA, USA). During the sampling cruise in the southern sea off Korea, Typhoon Bolaven, which was classified as Category 4, passed through this study region from 27 to 28 August 2012.

FDOM analysis. Seawater samples were vacuum-filtered using pre-combusted (450 °C for 4 h) GF/F filters (Whatman, pore size: 0.7 μm). Filtered samples were stored in pre-combusted dark-colored glass bottles. 3D fluorescence spectroscopy was conducted using a fluorescence spectrometer (FS-2, SCINCO, Korea) within 2 weeks after sampling. Excitation-emission matrix spectroscopy (EEMS) analysis was conducted by detecting emission wavelengths (Em) of 250–600 nm at 2-nm intervals, and excitation wavelengths (Ex) of 250–500 nm at 5-nm intervals. The slit widths were set to 10 nm for both excitation and emission monochromators, and the integration time was 50 ms. To prevent any artificial problems with the blank subtraction method, Rayleigh and Raman scatter bands (± 15 nm) were eliminated and replaced by the 3D Delaunay interpolation of the remaining adjacent data⁴⁸. The PARAFAC model was applied to identify the peaks of the specific individual fluorophores from 3D EEMS data⁴⁹. PARAFAC analysis for 249 EEMS data was performed using the MATLAB program R2015a (MathWorks, MA, USA) with the DOMFluor toolbox developed by Stedmon and Bro⁵⁰. The three components were statistically validated by split-half analysis (Figure S1). Fluorescence intensities of samples were normalized daily to fluorescence of a quinine sulfate dihydrate (QSU; μg QS/L) diluted in 0.1 N sulfuric acid at a specific wavelength (Ex/Em = 350/450 nm). The variation of its fluorescence was less than 3% of the average value throughout the all measurements. The precision of the measurements was ± 0.01 QSU, and the limit of quantification was 0.14 QSU⁹. The inner filter effect was not corrected because this artifact was negligible for various water samples using the spectrofluorometer^{51,52}.

Ra-228 analysis. The bulk seawater samples (~100 L) were passed through a column of MnO₂ impregnated acrylic fiber (Mn-fiber) at $<1 \text{ L min}^{-1}$ to extract Ra isotopes⁵³. Mn-fiber samples were hand-rinsed gently to remove any salts and ashed using a muffle furnace at 820 °C for 16 h. The ash was homogenized and transferred to hermetically sealed vials. The samples were then analyzed using a high-purity Germanium well-type detector (CANBERRA Industries Inc., Meriden, CT, USA). The activities for ²²⁸Ra were determined using the gamma peaks of ²²⁸Ac (at 911 keV)⁵⁴. Radium activities for all samples were corrected for radioactive decay to the sampling time. Uncertainties of radium isotope activities were computed using an error propagation calculation.

Data compilation. We also compiled data for ²²⁸Ra and surface FDOM during the summer season which have been documented from Lee *et al.*³⁹ and Kim and Kim¹⁴, respectively in order to strengthen our arguments. In the case of the FDOM data, the PARAFAC model was re-applied with the compiled raw data set of both seasons.

Data availability. The datasets analysed during the current study are available from the corresponding author upon reasonable request.

References

- Nelson, N. B. & Siegel, D. A. The Global Distribution and Dynamics of Chromophoric Dissolved Organic Matter. *Annual review of marine science* **5**, 447–476. <https://doi.org/10.1146/annurev-marine-120710-100751> (2013).
- Siegel, D., Maritorena, S., Nelson, N., Hansell, D. & Lorenzi-Kayser, M. Global distribution and dynamics of colored dissolved and detrital organic materials. *Journal of Geophysical Research* **107**, 3228 (2002).

3. Siegel, D., Maritorena, S., Nelson, N., Behrenfeld, M. & McClain, C. Colored dissolved organic matter and its influence on the satellite-based characterization of the ocean biosphere. *Geophysical Research Letters* **32** (2005).
4. Zepp, R. G., Erickson Iii, D. J., Paul, N. D. & Sulzberger, B. Interactive effects of solar UV radiation and climate change on biogeochemical cycling. *Photochemical & Photobiological Sciences* **6**, 286–300, <https://doi.org/10.1039/B700021A> (2007).
5. Blough, N. V. & Del Vecchio, R. In *Biogeochemistry of marine dissolved organic matter* (eds Dennis A. Hansel & Craig A. Carlson) Ch. Chromophoric DOM in the coastal environment, 509–546 (Academic Press, 2002).
6. Mopper, K. & Kieber, D. J. Marine photochemistry and its impact on carbon cycling. *The effects of UV radiation in the marine environment* **10**, 101–129 (2000).
7. Stedmon, C. A. & Nelson, N. B. In *Biogeochemistry of Marine Dissolved Organic Matter (Second Edition)* (eds Dennis A. Hansell & Craig A. Carlson) Ch. The Optical Properties of DOM in the Ocean, 481–508 (Academic Press, 2015).
8. Fichot, C. G. & Benner, R. The spectral slope coefficient of chromophoric dissolved organic matter ($S_{275-295}$) as a tracer of terrigenous dissolved organic carbon in river-influenced ocean margins. *Limnology and Oceanography* **57**, 1453–1466, <https://doi.org/10.4319/lo.2012.57.5.1453> (2012).
9. Kim, J. & Kim, G. Significant anaerobic production of fluorescent dissolved organic matter in the deep East Sea (Sea of Japan). *Geophysical Research Letters*, <https://doi.org/10.1002/2016GL069335> (2016).
10. Burdige, D. J., Kline, S. W. & Chen, W. Fluorescent dissolved organic matter in marine sediment pore waters. *Marine Chemistry* **89**, 289–311, <https://doi.org/10.1016/j.marchem.2004.02.015> (2004).
11. Chen, R. F., Bada, J. L. & Suzuki, Y. The relationship between dissolved organic carbon (DOC) and fluorescence in anoxic marine porewaters: Implications for estimating benthic DOC fluxes. *Geochimica et Cosmochimica Acta* **57**, 2149–2153, [https://doi.org/10.1016/0016-7037\(93\)90102-3](https://doi.org/10.1016/0016-7037(93)90102-3) (1993).
12. Skoog, A. *et al.* Early diagenetic production and sediment-water exchange of fluorescent dissolved organic matter in the coastal environment. *Geochimica et Cosmochimica Acta* **60**, 3619–3629, [https://doi.org/10.1016/0016-7037\(96\)83275-3](https://doi.org/10.1016/0016-7037(96)83275-3) (1996).
13. Yamashita, Y. & Tanoue, E. Production of bio-refractory fluorescent dissolved organic matter in the ocean interior. *Nature Geoscience* **1**, 579–582, <https://doi.org/10.1038/ngeo279> (2008).
14. Kim, J. & Kim, G. Importance of colored dissolved organic matter (CDOM) inputs from the deep sea to the euphotic zone: Results from the East (Japan) Sea. *Marine Chemistry* **169**, 33–40, <https://doi.org/10.1016/j.marchem.2014.12.010> (2015).
15. Wang, S.-L., Arthur Chen, C.-T., Hong, G.-H. & Chung, C.-S. Carbon dioxide and related parameters in the East China Sea. *Continental Shelf Research* **20**, 525–544, [https://doi.org/10.1016/S0278-4343\(99\)00084-9](https://doi.org/10.1016/S0278-4343(99)00084-9) (2000).
16. Isobe, A. *et al.* Freshwater and temperature transports through the Tsushima-Korea Straits. *Journal of Geophysical Research: Oceans* **107**, 2–1 (2002).
17. Chu, P. C., Fralick, C. R., Haeger, S. D. & Carron, M. J. A parametric model for the Yellow Sea thermal variability. *Journal of Geophysical Research: Oceans* **102**, 10499–10507, <https://doi.org/10.1029/97JC00444> (1997).
18. Chang, P. H. *et al.* Summer behavior of the Changjiang diluted water to the East/Japan Sea: A modeling study in 2003. *Continental Shelf Research* **81**, 7–18, <https://doi.org/10.1016/j.csr.2014.03.007> (2014).
19. Chang, P. H. & Isobe, A. A numerical study on the Changjiang diluted water in the Yellow and East China Seas. *Journal of Geophysical Research: Oceans* **108**, 15–11, <https://doi.org/10.1029/2002JC001749> (2003).
20. Lie, H. J., Cho, C. H., Lee, J. H. & Lee, S. Structure and eastward extension of the Changjiang River plume in the East China Sea. *Journal of Geophysical Research-Oceans* **108**, <https://doi.org/10.1029/2001jc001194> (2003).
21. Yang, S. L., Zhang, J. & Xu, X. J. Influence of the Three Gorges Dam on downstream delivery of sediment and its environmental implications, Yangtze River. *Geophysical Research Letters* **34**, n/a–n/a, <https://doi.org/10.1029/2007GL029472> (2007).
22. Gong, G.-C. *et al.* Reduction of primary production and changing of nutrient ratio in the East China Sea: Effect of the Three Gorges Dam? *Geophysical Research Letters* **33**, n/a–n/a, <https://doi.org/10.1029/2006GL025800> (2006).
23. Yang, Z. *et al.* Dam impacts on the Changjiang (Yangtze) River sediment discharge to the sea: The past 55 years and after the Three Gorges Dam. *Water Resources Research* **42**, n/a–n/a, <https://doi.org/10.1029/2005WR003970> (2006).
24. Guo, L. & He, Q. Freshwater flocculation of suspended sediments in the Yangtze River, China. *Ocean Dynamics* **61**, 371–386, <https://doi.org/10.1007/s10236-011-0391-x> (2011).
25. Guo, W. *et al.* The conservative and non-conservative behavior of chromophoric dissolved organic matter in Chinese estuarine waters. *Marine Chemistry* **107**, 357–366, <https://doi.org/10.1016/j.marchem.2007.03.006> (2007).
26. Bai, Y., Su, R. & Shi, X. Assessing the dynamics of chromophoric dissolved organic matter in the southern Yellow Sea by excitation-emission matrix fluorescence and parallel factor analysis (EEM-PARAFAC). *Continental Shelf Research* **88**, 103–116, <https://doi.org/10.1016/j.csr.2014.07.011> (2014).
27. Su, R., Bai, Y., Zhang, C. & Shi, X. The assessment of the spatial and seasonal variability of chromophoric dissolved organic matter in the Southern Yellow Sea and the East China Sea. *Marine Pollution Bulletin* **100**, 523–533, <https://doi.org/10.1016/j.marpolbul.2015.09.002> (2015).
28. Coble, P. G. Characterization of marine and terrestrial DOM in seawater using excitation-emission matrix spectroscopy. *Marine Chemistry* **51**, 325–346 (1996).
29. Murphy, K. R., Stedmon, C. A., Waite, T. D. & Ruiz, G. M. Distinguishing between terrestrial and autochthonous organic matter sources in marine environments using fluorescence spectroscopy. *Marine Chemistry* **108**, 40–58 (2008).
30. Clark, C. D., Litz, L. P. & Grant, S. B. Saltmarshes as a source of chromophoric dissolved organic matter (CDOM) to Southern California coastal waters. *Limnology and Oceanography* **53**, 1923–1933, <https://doi.org/10.4319/lo.2008.53.5.1923> (2008).
31. Yamashita, Y. & Tanoue, E. Chemical characterization of protein-like fluorophores in DOM in relation to aromatic amino acids. *Marine Chemistry* **82**, 255–271, [https://doi.org/10.1016/S0304-4203\(03\)00073-2](https://doi.org/10.1016/S0304-4203(03)00073-2) (2003).
32. Baker, A. & Spencer, R. G. M. Characterization of dissolved organic matter from source to sea using fluorescence and absorbance spectroscopy. *Science of the Total Environment* **333**, 217–232, <https://doi.org/10.1016/j.scitotenv.2004.04.013> (2004).
33. Osburn, C. L., Mikan, M. P., Etheridge, J. R., Burchell, M. R. & Birgand, F. Seasonal variation in the quality of dissolved and particulate organic matter exchanged between a salt marsh and its adjacent estuary. *Journal of Geophysical Research: Biogeosciences* **120**, 1430–1449, <https://doi.org/10.1002/2014JG002897> (2015).
34. Jørgensen, L. *et al.* Global trends in the fluorescence characteristics and distribution of marine dissolved organic matter. *Marine Chemistry* **126**, 139–148, <https://doi.org/10.1016/j.marchem.2011.05.002> (2011).
35. Zhang, L. *et al.* The spatiotemporal distribution of dissolved inorganic and organic carbon in the main stem of the Changjiang (Yangtze) River and the effect of the Three Gorges Reservoir. *Journal of Geophysical Research: Biogeosciences* **119**, 2012JG002230, <https://doi.org/10.1002/2012JG002230> (2014).
36. Gao, L., Fan, D., Sun, C., Li, D. & Cai, J. Optical characterization of CDOM in a marsh-influenced environment in the Changjiang (Yangtze River) Estuary. *Environmental Earth Sciences* **64**, 643–658, <https://doi.org/10.1007/s12665-010-0885-8> (2011).
37. Lie, H.-J. & Cho, C.-H. Seasonal circulation patterns of the Yellow and East China Seas derived from satellite-tracked drifter trajectories and hydrographic observations. *Progress in Oceanography* **146**, 121–141, <https://doi.org/10.1016/j.pocean.2016.06.004> (2016).
38. Kim, G., Ryu, J.-W., Yang, H.-S. & Yun, S.-T. Submarine groundwater discharge (SGD) into the Yellow Sea revealed by ^{228}Ra and ^{226}Ra isotopes: Implications for global silicate fluxes. *Earth and Planetary Science Letters* **237**, 156–166 (2005).

39. Lee, H., Kim, G., Kim, J., Park, G. & Song, K.-H. Tracing the flow rate and mixing ratio of the Changjiang diluted water in the northwestern Pacific marginal seas using radium isotopes. *Geophysical Research Letters* **41**, 2014GL060230, <https://doi.org/10.1002/2014GL060230> (2014).
40. Nozaki, Y., Tsubota, H., Kasemsupaya, V., Yashima, M. & Naoko, I. Residence times of surface water and particle-reactive ^{210}Pb and ^{210}Po in the East China and Yellow seas. *Geochimica et Cosmochimica Acta* **55**, 1265–1272 (1991).
41. Xu, B.-C., Dimova, N. T., Zhao, L., Jiang, X.-Y. & Yu, Z.-G. Determination of water ages and flushing rates using short-lived radium isotopes in large estuarine system, the Yangtze River Estuary, China. *Estuarine, Coastal and Shelf Science* **121–122**, 61–68, <https://doi.org/10.1016/j.ecss.2013.02.005> (2013).
42. Wang, Y., Zhang, D., Shen, Z., Feng, C. & Chen, J. Revealing Sources and Distribution Changes of Dissolved Organic Matter (DOM) in Pore Water of Sediment from the Yangtze Estuary. *PLoS ONE* **8**, e76633, <https://doi.org/10.1371/journal.pone.0076633> (2013).
43. Gao, L., Fan, D., Li, D. & Cai, J. Fluorescence characteristics of chromophoric dissolved organic matter in shallow water along the Zhejiang coasts, southeast China. *Marine Environmental Research* **69**, 187–197, <https://doi.org/10.1016/j.marenvres.2009.10.004> (2010).
44. Wang, B.-d., Wang, X.-l. & Zhan, R. Nutrient conditions in the Yellow Sea and the East China Sea. *Estuarine, Coastal and Shelf Science* **58**, 127–136, [https://doi.org/10.1016/S0272-7714\(03\)00067-2](https://doi.org/10.1016/S0272-7714(03)00067-2) (2003).
45. Chen, C.-T. A. Distributions of nutrients in the East China Sea and the South China Sea connection. *Journal of Oceanography* **64**, 737–751, <https://doi.org/10.1007/s10872-008-0062-9> (2008).
46. Hoge, F. E. & Lyon, P. E. Satellite observation of Chromophoric Dissolved Organic Matter (CDOM) variability in the wake of hurricanes and typhoons. *Geophysical Research Letters* **29**, 14-11–14-14, <https://doi.org/10.1029/2002GL015114> (2002).
47. Boss, E., Pegau, W. S., Zaneveld, J. R. V. & Barnard, A. H. Spatial and temporal variability of absorption by dissolved material at a continental shelf. *Journal of Geophysical Research: Oceans* **106**, 9499–9507, <https://doi.org/10.1029/2000JC900008> (2001).
48. Zepp, R. G., Sheldon, W. M. & Moran, M. A. Dissolved organic fluorophores in southeastern US coastal waters: Correction method for eliminating Rayleigh and Raman scattering peaks in excitation-emission matrices. *Marine Chemistry* **89**, 15–36, <https://doi.org/10.1016/j.marchem.2004.02.006> (2004).
49. Stedmon, C. A., Markager, S. & Bro, R. Tracing dissolved organic matter in aquatic environments using a new approach to fluorescence spectroscopy. *Marine Chemistry* **82**, 239–254 (2003).
50. Stedmon, C. A. & Bro, R. Characterizing dissolved organic matter fluorescence with parallel factor analysis: A tutorial. *Limnology and Oceanography: Methods* **6**, 572–579 (2008).
51. Kim, J. & Kim, G. Inputs of humic fluorescent dissolved organic matter via submarine groundwater discharge to coastal waters off a volcanic island (Jeju, Korea). *Scientific Reports* **7**, 7921, <https://doi.org/10.1038/s41598-017-08518-5> (2017).
52. Yan, G. & Kim, G. Speciation and Sources of Brown Carbon in Precipitation at Seoul, Korea: Insights from Excitation–Emission Matrix Spectroscopy and Carbon Isotopic Analysis. *Environmental science & technology*, <https://doi.org/10.1021/acs.est.7b02892> (2017).
53. Moore, W. S. Sampling ^{228}Ra in the deep ocean. *Deep Sea Research and Oceanographic Abstracts* **23**, 647–651, [https://doi.org/10.1016/0011-7471\(76\)90007-3](https://doi.org/10.1016/0011-7471(76)90007-3) (1976).
54. Kim, G., Lee, K.-K., Park, K.-S., Hwang, D.-W. & Yang, H.-S. Large submarine groundwater discharge (SGD) from a volcanic island. *Geophysical Research Letters* **30**, 2098, <https://doi.org/10.1029/2003GL018378> (2003).

Acknowledgements

We would like to thank Dr. Gwanserk Park of the KCG Research Institute and Hojun Lee of the Republic of Korea Naval Academy for helping in the collection of seawater samples during the sampling campaigns. We would also like to thank the captains and the crew members of R/V Tamgu-3 and R/V Tamgu-8 of the National Institute of Fisheries Science (NIFS), of KCG vessel 3011 of the KCG, and of R/V Eardo and R/V Onnuri of the KIOST for their assistance during the sampling cruises. Data supporting figures and calculations in the manuscript are included in the table in the supporting information. This research was funded by the National Research Foundation (NRF) of Korea (NRF-2015R1A2A1A10054309) and by the project titled “Deep Water Circulation and Material Cycling in the EAST Sea (2016)”, funded by the Ministry of Oceans and Fisheries, Korea.

Author Contributions

J.K. performed sampling, chemical analysis, PARAFAC modeling, and calculation under the supervision of G.K. J.K. and G.K. wrote the manuscript. H.M.C. contributed to the sample collection and analysis of ^{228}Ra for the sampling cruise in February 2017.

Additional Information

Supplementary information accompanies this paper at <https://doi.org/10.1038/s41598-018-23299-1>.

Competing Interests: The authors declare no competing interests.

Publisher's note: Springer Nature remains neutral with regard to jurisdictional claims in published maps and institutional affiliations.



Open Access This article is licensed under a Creative Commons Attribution 4.0 International License, which permits use, sharing, adaptation, distribution and reproduction in any medium or format, as long as you give appropriate credit to the original author(s) and the source, provide a link to the Creative Commons license, and indicate if changes were made. The images or other third party material in this article are included in the article's Creative Commons license, unless indicated otherwise in a credit line to the material. If material is not included in the article's Creative Commons license and your intended use is not permitted by statutory regulation or exceeds the permitted use, you will need to obtain permission directly from the copyright holder. To view a copy of this license, visit <http://creativecommons.org/licenses/by/4.0/>.

© The Author(s) 2018